Contents lists available at SciOpen

Food Science and Human Wellness

journal homepage: https://www.sciopen.com/journal/2097-0765

China Food Publishing Co.

Isodon Suzhouensis extract interferes with miRNA expression profile for prevention and treatment of chronic obstructive pneumonia disease

Hong Duan[a,b,c,1], Han Li[a,b,1], Jun Feng[a], Jing Zhou[a,b], Ying Shi[a,b], Li Wang[a,c], Zeng Dong[a], Kefeng Zhai[a,b,*], Henggui Hu[d,*], Zhaojun Wei[e,*]

[a] *School of Biological and Food Engineering, Engineering Research Center for Development and High Value Utilization of Genuine Medicinal Materials in North Anhui Province, Suzhou University, Suzhou 234000, China*
[b] *College of Biological and Food Engineering, Anhui Polytechnic University, Wuhu 241000, China*
[c] *College of Pharmacy, Xinjiang Medical University, Urumqi 830000, China*
[d] *General Clinical Research Center, Anhui Wanbei Coal-Electricity Group General Hospital, Suzhou 234000, China*
[e] *School of Biological Science and Engineering, North Minzu University, Yinchuan 750021, China*

ARTICLE INFO

Article history:
Received 6 March 2024
Received in revised form 19 March 2024
Accepted 28 March 2024

Keywords:
Chronic obstructive pulmonary disease
microRNA
Biomarker
High-throughput sequencing
Isodon Suzhouensis leaf extract

ABSTRACT

Chronic obstructive pulmonary disease (COPD) is a respiratory condition characterized by several symptoms. The pathogenesis of COPD is complex and involves multiple factors. A fantastic drug from traditional Chinese medicine, *Isodon Suzhouensis* (ISZ) is a perennial herb belonging to the Labiaceae family. It has the functions of resolving phlegm, removing stasis, promoting blood circulation and eliminating qi stagnation. ISZ has been found to possess great potential against COPD. Present study is focused on identifying microRNA (miRNA) biomarkers for COPD and determining the role of ISZ leaf extract in regulating the disease through miRNA expression in serum exosomes. The Sprague Dawley (SD) rats were randomly divided into control group, COPD group and COPD + ISZ group. After the establishment of the model, the rats were sacrificed, and the results were compared with the control group. Then the total RNA of rat serum was extracted and identified by nanoparticle tracker. Finally, high-throughput screening and sequencing were performed to screen miRNAs with significant differential expression. Then, different databases were used to figure out the possible target genes, and their functions were assessed by employing Gene Ontology (GO) as well as Kyoto Encyclopedia of Genes and Genomes (KEGG) analyses. The sequencing results were then further verified by qRT-PCR. The results pointed out that these 17 differentially expressed miRNAs may have the potential of diagnostic and prognostic biomarkers against COPD. Interestingly, it was also found that ISZ leaf extract may regulate the occurrence of COPD by affecting the expression of miRNAs. This study identified the biomarkers of COPD and clarified the mechanism of the treatment of COPD by ISZ leaf extract, which is helpful to improve the level of early diagnosis and treatment of COPD.

1. Introduction

Chronic obstructive pulmonary pneumonia (COPD) is the leading cause of death and morbidity of chronic diseases worldwide, which imposes a heavy burden on society the economy[1]. It is a preventable and treatable respiratory disease in which the reaction of harmful particles or gases can lead to chronic airway inflammation in the lungs[2-3].

[1] These authors contributed equally to this work.
[*] Corresponding authors.
E-mail address: kefengzhai@163.com (K.F. Zhai); huhenggui@163.com (H.G. Hu); zjwei@hfut.edu.cn (Z.J. Wei)
Peer review under responsibility of Beijing Academy of Food Sciences.

Publishing services by Tsinghua University Press

http://doi.org/10.26599/FSHW.2024.9250250

COPD is characterized by dyspnea, chronic cough, and sputum, is a disease with complex pathogenesis[4]. It can further develop into pulmonary heart disease and respiratory failure, which is a common chronic disease[5]. Technically, COPD is associated with abnormal inflammatory reactions of harmful hazardous gases and particles with high disability and fatality rates[6]. The global incidence rate of over-40-year-olds has reached 9%–10%. Because of the complex pathophysiology and extreme variations of COPD, its pathogenesis remains unclear[7].

Exosomes are small membrane vesicles (30–200 nm) containing complex RNAs and proteins that play an important role in cellular interactions. The release of microRNA (miRNA) by exosomes is an important mechanism of genetic exchange between the cells[8]. As a regulatory factor of gene expression, miRNA is highly stable in serum or plasma and is a promising biomarker, so there is increasing hope for its future use as a biomarker[9-10]. Recent studies of circulating miRNAs in plasma, serum, and other body fluids have shown that circulating miRNAs are not digested by RNase and remain stable at high pH after boiling and multiple freeze-thaw cycles[11]. miRNAs regulate a wide range of diseases, such as atherosclerosis (AS)[12], oral squamous cell carcinoma (OSCC)[13], and nasopharyngeal carcinoma (NPC)[14]. Most cellular processes and pathways can be regulated by negatively affecting the protein expression of multiple target genes. These small non-coding RNAs play an important role in a variety of human diseases[15]. Multiple miRNAs are involved in the regulation of COPD lesions, suggesting that miRNAs can be used as biomarkers of COPD[16]. To detect COPD earlier and more accurately, there is a dire need for the identification of precise biomarkers for the diagnosis and prognosis of COPD.

As a traditional Chinese herbal medicine in Suzhou area, *Isodon Suzhouensis* (ISZ) is a perennial herb belonging to the Labiaceae family. It has the functions of resolving phlegm and dispersing congealing, promoting blood circulation and removing stagnation of qi, etc.[17]. The taste is bitter, it has the effect of reducing lung qi, relieving cough and panting, treating Yang heat and syndrome of deficiency and accumulation. It has the effect of clearing heat, purging fire, cooling blood and antipyretic poison. There is a folk tradition of taking ISZ decoction to cure diseases. It is used to treat chronic bronchitis, COPD, lung abscess, chronic osteomyelitis, boil abscess, tonsillitis, sepsis, etc., and has achieved good results[18-19]. Earlier studies have reported that the extract of ISZ contains a large number of flavonoids and diterpenoids[20]. The discovery of a large number of potential miRNAs biomarkers of chronic obstructive disease as well as the interventional studies of ISZ leaves extract showed that flavonoids have the role of strong antioxidants under normal conditions as well as pathological oxidative conditions, can activate apoptosis, inhibit proliferation and inflammation, and possess strong immunomodulatory effects. Terpenoids have also been found involved in many cancerous diseases. Additionally, earlier published studies have reported the strong potential of ISZ in the regulation and improvement of COPD[17].

2. Material and methods

2.1 Preparation of extracts from ISZ

ISZ was purchased from Suzhou Lvyuan Traditional Chinese Medicine Technology Co., Ltd. (Suzhou, China). The specific extraction methods refer to Wang et al.[17]. In brief, the dried ISZ is crushed through an 80 mesh sieve, using ultrasonic extraction method to prepare ISZ leaf extract.

2.2 Animal and chronic obstructive pulmonary disease model

Specific pathogen free (SPF) grade Sprague Dawley (SD) male rats (8 weeks old, weight (200 ± 20) g) were purchased from Anhui Medical University. Animals were kept at a standard temperature of (22 ± 2) ℃, relative humidity of 55%–65%, and a 12 h light/12 h dark cycle. A total of 36 male SD rats were randomly divided into 6 groups: control group (K1, K2), COPD group (M1, M2), and COPD + ISZ group (D1, D2), with 6 animals in each group. COPD model was established by nasal inhalation of lipopolysaccharide (LPS) and smoking in rats[21]. The experiment began after 3 days of adaptive feeding. The control group was not fumigated. The COPD group and COPD + ISZ group were fumigated once every 8 h, twice a day, passive smoking of 10 cigarettes per time, exposure time of 30 min, and a total of 28 days. LPS 0.2 mL (200 μg) was inhaled intranasally on days 1 and 14, and no fumigation was performed on the same day. Feed normally the rest of the time. Drug intervention was initiated on the 15th day of modeling. The COPD + ISZ group was intragastrically given ISZ leaves extract 150 mg/kg, and the control group and COPD group were intragastrically given normal saline 10 mL/kg for 14 days. Rat drinking water was disinfected with ultraviolet light, and water bottles and pads were replaced every other day. On day 28, the rats were anesthetized with chloral hydrate solution (10% concentration) by standard intraperitoneal injection of 0.6 mL/100 g. The rats were transferred to the anatomic table and fixed in the supine position. Make a quick abdominal incision along the midline to collect aortic blood. After the rats had been killed, the right lung was cut along the hilum. All animal handling procedures followed the application of Suzhou University Laboratory Animal Management Guidelines (SZU-19002).

2.3 Hematoxylin and eosin (HE) staining

The right lung tissue was taken, rinsed with PBS buffer solution, cut 0.2 cm × 0.2 cm, fixed with Tissue-Tek O.C.T. compound (Sakura Finetek Co., Ltd., Tokyo, Japan) embedding glue, frozen, and processed into slices with thickness of 8 μm, which were stuck on the slide, namely, the preparation process was completed, and HE staining (Yi Fei Xue Biotechnology Co., Ltd., Nanjing, China)[22] was performed.

HE staining procedure: frozen sections were fixed with paraformaldehyde for 30 min and washed with PBS; Hematoxylin was stained for 5–10 s, rinsed with PBS, treated with 1% hydrochloric acid ethanol differentiated solution for 5–10 s, rinsed with PBS, and dyed with eosin for 1 min. Rinse with PBS and cover with cover glass. The histopathological changes were observed under a light microscope.

2.4 Isolation and identification of exosomes

The blood from arteries was drawn and stored in the refrigerator (4 ℃) for a couple of hours and then centrifuged at 2 500 × *g* for 15 min for serum isolation. The obtained serum as supernatant was then subjected to total exosome isolation by Thermo Fisher

Scientific (MA, USA) as per briefed instructions of the manufacturer. The morphological assessment of the obtained exosomes was assessed by transmission electron microscopic technique (TEM; JEM-1200EX, Japan) as per manufacturer's specifications revised by Rodriguez-Caro and Dragovic[23]. Exosomes (10 μL) were incubated for 10 min at room temperature on a copper grid, stained with aqueous uranyl acetate (2%), and then air dried. The sample was then examined by TEM. Nanoparticle tracking analysis (NTA) was employed for the assessment of the size of exosomes with the utility of Zetaview (Particle Metrix) at a wavelength of 488 nm. For this particle size assessment, the samples were diluted with PBS, and the final input dilution was 1:1 000 as recommended by the Zitaview (Particle Metrix) manufacturer, while the prevalence of particular exosomes was further assessed *via* Western blotting for which the isolated exosomes were nurtured with cell lysate buffer[24]. The used primary antibodies CD9 for this Western blot were obtained from Cell Signaling Technology (Beverly, MA, USA), while the secondary antibodies were obtained from Bioworld Technology INC (MN, USA). The reactive protein bands were obtained on polyvinylidene difloride (PVDF) membrane and were accordingly visualized using FluorChemHD2 Imaging system (Protein Simple, CA, USA). The intensities of obtained bands were assessed *via* Alpha View SA software as briefly described by previous studies[12,23].

2.5 RNA extraction

Extraction of serum exosome miRNA was done by express miRNA extraction kit (Tissue&Cell, HaiGene Co., Ltd., Harbin, China). The specific extraction methods was adapted from Zhai et al.[12]. In brief, the exosome suspension was obtained, and 300 μL miRNA reagent A was added to the sample, which was shaken vigorously and then allowed to settle down for 5 min at room temperature. Then, 300 μL of miRNA reagent B was added with gentle mixing of solutions. Afterward, the solution was centrifuged at 13 400 × *g* for 5 min, and about 550 μL supernatant was transferred into a new 1.5 mL EP tube. Further, 200 μL anhydrous ethanol was added into the supernatant with thorough mixing, then allowed to settle down for 5 min at room temperature. The EP tube was then centrifuged again at 13 400 × *g* for 10 min, 700 μL supernatant was transferred to a 1.5 mL EP tube, along with a vigorous addition of 300 μL isopropyl alcohol. The finally formulated solution was then transferred into adsorption column and centrifuged at 13 400 × *g* for 1 min out of which the filtrate was separated and 700 μL of 75% isopropyl alcohol was dripped into the adsorption column for washing, then centrifuged at 13 400 × *g* for 1 min after which the filtrate separated away, another 500 μL anhydrous ethanol was added into the adsorption column after careful washing, then centrifuged (13 400 × *g*, 1 min) and poured away the filtrate. The adsorption column was centrifuged at 13 400 × *g* for 2 min to remove the residual ethanol. The adsorption column was placed in a new 1.5 mL EP tube and placed at room temperature for 2 min for the complete evaporation of ethanol. RNase Free TE Buffer was then added into the filter element of the adsorption column, placed at room temperature for 2 min, and centrifuged at 13 400 × *g* for 2 min, and the elution product was the extracted miRNA.

2.6 Screening significant differential miRNAs

The total RNAs from 6 samples were extracted for sequencing. HiSeq2000 deep sequencing technology (Shenzhen BGI Co., Ltd., Wuhan, China). Constructed a small RNA library and constructed a cDNA library. miRNAs were sequenced using next-generation high-throughput sequencing techniques[25]. Briefly, the raw sequencing data is obtained using the Illumina HiSeq2000 sequencer (BGI), which is then mapped to small RNA databases, including siRNA, RNase, RFAM, siRNA, snoRNA, and other databases used to classify annotations.

2.7 Bioinformatics analysis

To pinpoint the differentially expressed miRNA targets, several different types of software of the latest available versions were used for the bioinformatic analyses including RNAhybrid, miRNAda, and TargetScan. The pointed findings were then statistically analyzed ($P \leq 0.05$), and the finalized miRNA were then further subjected to Gene Ontology (GO) and Kyoto Encyclopedia of Genes and Genomes (KEGG) pathway analysis.

2.8 Confirmation of expression of miRNAs

From deep sequencing and bioinformatic tools, resultantly obtained differentially expressed miRNAs were further verified with *in vitro* experimentation. The COPD associated shortlisted miRNAs were then analyzed *via* qRT-PCR as per the protocol followed by[26]. Express miRNA extraction kit (tissue and cell) was used for obtaining the miRNAs from the exosomes, while cDNA synthesis kit (Haigene Biotech, Harbin, China) was used for reverse transcription of RNAs. All of the studied samples were normalized and standardized as per the reference value of internal reference gene U6 snRNA, and the relative fold change (FC) was quantified in comparison to the internal reference gene for the analytical purpose (U6 snRNA) as described by previous studies[27-28].

2.9 Statistical analysis

The data were statistically analyzed using GraphPad Prism version 8.0 and expressed as mean ± standard error of mean (SEM). The difference between the two groups was evaluated by Student's *t*-test. $P < 0.05$ and $P < 0.01$ were considered statistically significant.

3. Results

3.1 Pathological changes of lung tissue of rats in each group

The results of HE staining showed that there was a little inflammatory cell infiltration in the lung tissue of rats in the control group, the alveolar epithelium and bronchial wall were intact, and no obvious mucosal edema or alveolar destruction was observed in Fig. 1A. In the COPD group, the bronchial wall of lung tissue was thickened, a large number of inflammatory cells were attached, the trachea mucosal epithelium was necrotic, and the alveolar structure was disturbed (Fig. 1B). The pulmonary histopathology of rats in the COPD + ISZ group was improved to a certain extent, and the bronchial wall was significantly thinner, the invasion of inflammatory

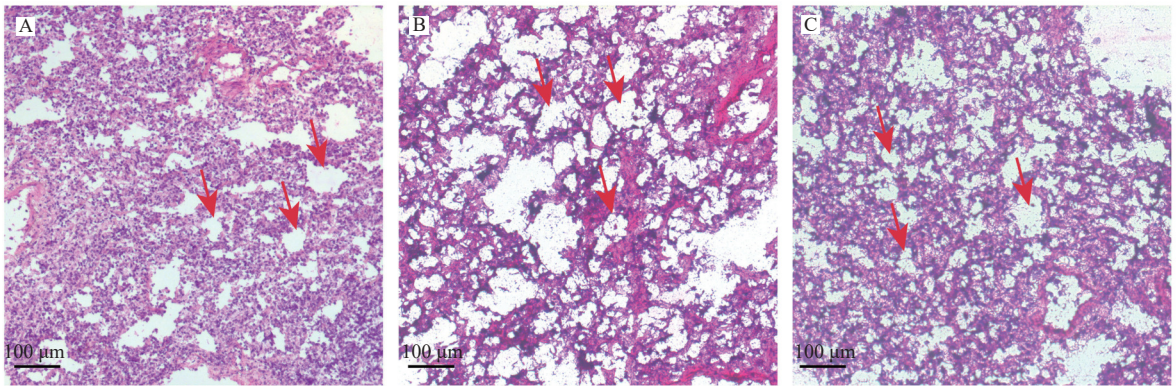

Fig. 1 Representative HE staining of lung tissue sections (×200). (A) Control group. (B) COPD group. (C) COPD + ISZ group. $n = 6$.

cells was reduced, and the destruction of alveolar septum was lighter than that in the COPD group (Fig. 1C). These results indicate that ISZ can improve COPD.

3.2 Isolation and characterization of exosomes

Exosomes are small extracellular vesicles that play a crucial role in cell-to-cell communication. They are released by various cell types, including immune cells, stem cells, and tumor cells. Exosomes contain a diverse range of biomolecules, including proteins, lipids, nucleic acids (such as RNA and DNA), and signaling molecules. These vesicles are involved in intercellular communication by transferring their cargo to recipient cells. Exosomes are formed through the process of endocytosis, where a portion of the cell membrane invaginated and formed an intracellular vesicle called an endosome. These endosomes then mature and develop into multivesicular bodies (MVBs) within the cell. Eventually, these MVBs fuse with the cell membrane, releasing the internal vesicles (exosomes) into the extracellular space. Once released, exosomes can travel through bodily fluids, such as blood, urine, and cerebrospinal fluid, and reach distant target cells. They can bind to recipient cells and deliver cargo, thereby influencing various cellular processes, including cell differentiation, immune response modulation, and tissue repair[29]. Exosomes have gained significant attention in the field of biomedical research due to their potential applications in diagnostics and therapeutics. Their unique composition and ability to carry molecular cargo make them attractive candidates for various purposes. Exosomes derived from specific cell types can be isolated and analyzed to gain insights into disease progression or used as biomarkers for diagnostic purposes. Current studies are focusing on exploring the use of exosomes as delivery vehicles for therapeutics, including drugs, nucleic acids, and proteins, as they offer advantages such as improved stability, targeted delivery, and reduced immunogenicity. Our TEM analyses of exosome from the serum showed their irregularly circular to elliptical structures with wide variation in sizes ranging from 30 nm to 200 nm in diameter (Fig. 2A) for further clarity exosome specific biomarker CD9 was also analyzed *via* Western blotting (Fig. 2B). To

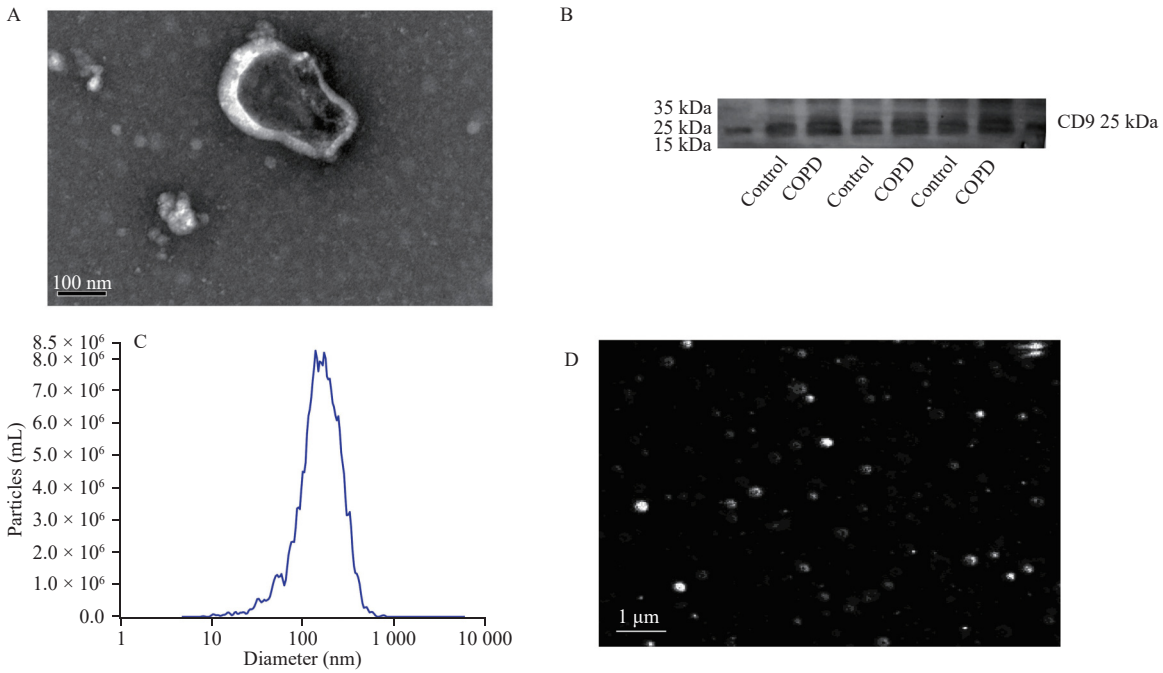

Fig. 2 Characterization of exosomes. (A) Representative TEM image of exosomes (scale bar 100 nm), $n = 6$. (B) Standard markers CD9 was detected by Western blot. (C) NTA of exosomes. (D) Video capture of recorded exosomes movements.

further verify whether the particles are isolated exosomes, an NTA test was also performed, which showed that their diameters were concentrated around 153.6 nm, corresponding to a local concentration of 7.9 × 10^6 particles/mL (Figs. 2C and D). These data showed that exosomes had been isolated from human serum successfully.

3.3 *miRNAs classification and annotation*

miRNAs annotation statistics are identified by comparison with known sRNA databases. To identify each miRNA having a unique annotation a priority sequence was followed with, miRNA > pi-RNA > snoRNA > R-fam > other sRNA. By comparing the classification annotation results of mature miRNAs in miRNA database, the mature information and precursor information of mature miRNAs were screened out[30]. The known miRNAs were identified by comparison with miRNA database. The statistical results of sequencing data volume in each group are shown in Table S1. The results of miRNA classification annotation are shown in Fig. 3.

Extract total RNA from 6 samples respectively, the preparation of the 6 cDNA libraries, respectively named K1, K2 (2 replicates of the control group), M1, M2 (2 replicates of the COPD group) and D1, D2 (2 replicates in the COPD + ISZ group), sequenced by sequencing Illumina depth of these libraries, and to filter the original sequencing readings. Each cDNA library for K1, K2; M1, M2; and D1 and D2 generated 25, 165 and 824 raw readings, respectively. The *Q*20 values of pure sequencing were 99.1%, 99.2% for K1 and K2; 99.2%, 99.3% for M1 and M2; and 99.1%, 99.2% for D1 and D2, respectively (Table 1). The resultant values of *Q*20 were consistently greater than 97% which is an indication of high-quality sequencing.

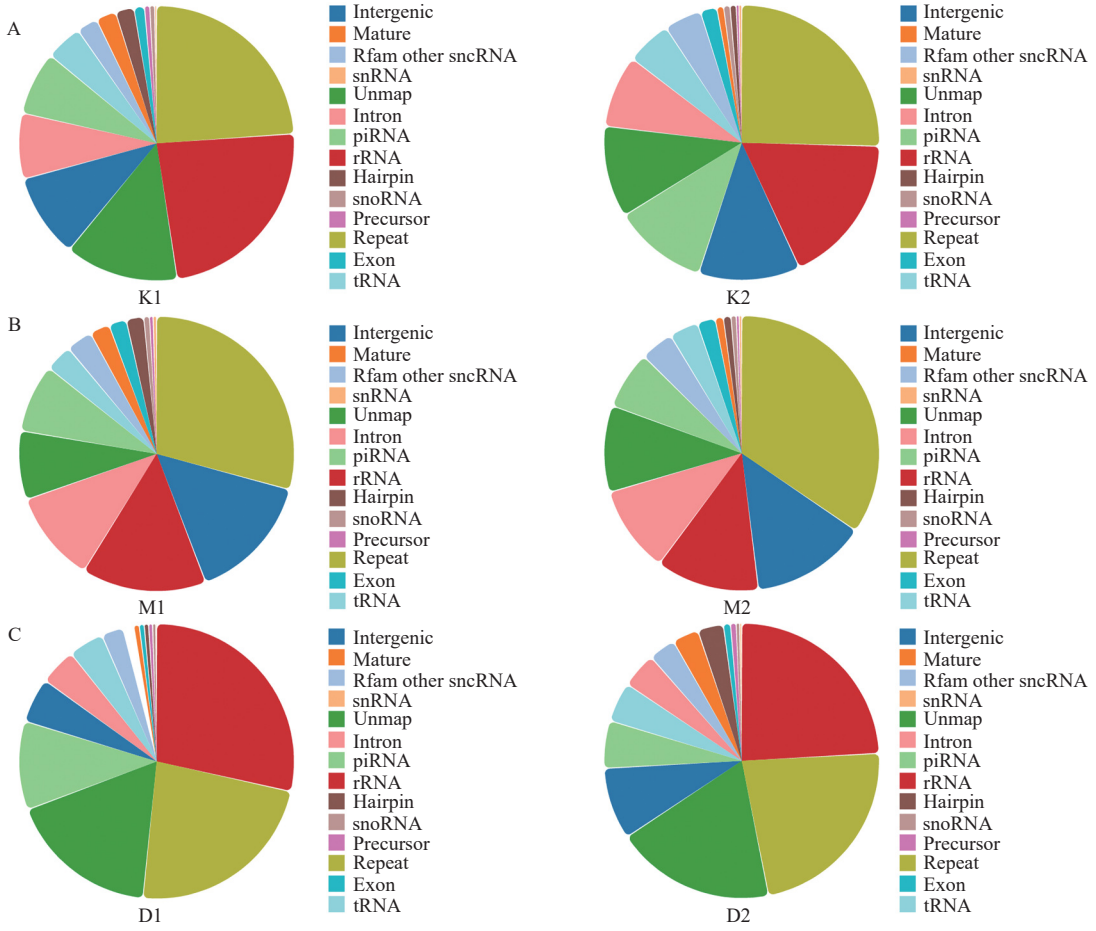

Fig. 3 miRNA classification annotation results. (A) K1 and K2 group (Control group); (B) M1 and M2 group (COPD group); (C) D1 and D2 group (COPD + ISZ group).

Table 1
Transcriptome data statistics (n = 6).

Sample	K1	K2	M1	M2	D1	D2
Raw tag count	25 165 824	25 165 824	25 165 824	25 165 824	25 165 824	25 165 824
Low quality tag count	456 952	456 249	414 291	447 712	379 842	448 796
Invalid adapter tag count	252 614	197 202	315 077	176 872	217 866	363 800
Poly A tag count	1 585	2 550	1 138	650	1 622	1 066
Short valid length tag	811 149	317 678	282 345	235 180	154 480	354 599
Clean tag count	23 643 524	24 192 145	24 152 973	24 305 410	24 412 014	23 997 563
*Q*20 of clean tag	99.1	99.2	99.2	99.3	99.1	99.2
Percentage of clean tag (%)	93.95	96.13	95.98	96.58	97.00	95.36

3.4 Screening for significantly different miRNAs

In this study, there were biological replicates in the control group (K1 and K2), the COPD group (M1 and M2), and the COPD + ISZ group (D1 and D2). The average expression level of the 2 biologically duplicated groups was taken for further study. In the COPD group and the control group, the miRNA expression contrast, 25 up-regulated miRNAs and 47 down-regulated miRNAs may be a biomarker of COPD ($P \leq 0.05$ and $|\log_2 FC| \geq 1$) (Table 2). In the comparison of miRNA expression profiles between the COPD group and the COPD + ISZ group, there were 34 up-regulated miRNAs and 44 down-regulated miRNAs (Table 3).

In order to confirm that the extract of ISZ regulates the disease by affecting the expression of serum exosomes, We further analyzed the co-intersecting cross miRNAs, a total of 32 miRNAs with significant differences were screened, among which 13 miRNAs were up-regulated and 19 were down-regulated ($|\log_2 FD (M/K)| \geq 1$, FDR < 0.001) (Table S2). A total of 17 miRNAs with significant differences were screened, including 4 up-regulated miRNAs and 13 down-regulated miRNAs ($|\log_2 FD (M/K)| \geq 2$, FDR < 0.001) (Tables S3 and S4).

3.5 Differential miRNA cluster analysis

The heatmap function in R software was applied to hierarchical clustering analysis. The clustering analysis results (Fig. 4) showed that 17 differentially expressed miRNAs could be correctly separated between the COPD group and the control group. Therefore, these 17 miRNAs may become biomarkers for the detection of COPD changes, and ISZ may improve COPD through their regulation.

3.6 Target gene prediction and functional analysis of miRNAs

Multiple software (miRANDA, TargetScan, and RNAHybrid) were used to predict target genes with significantly different miRNA expression. The statistical results of the number of target genes predicted

Table 2
miRNA was differentially expressed between the COPD group (M) and control group (K) (n =12).

Gene ID	$\log_2$ FC (M/K)	P-value (M/K)	Gene ID	$\log_2$ FC (M/K)	P-value (M/K)
rno-miR-106b-5p	5.519 87	0	rno-miR-193a-5p	–1.298 64	0.000 11
rno-miR-672-5p	5.230 36	0.000 01	rno-miR-411-5p	–1.335 91	0
rno-miR-190b-5p	5.147 90	0.000 02	rno-miR-15a-5p	–1.372 52	0
rno-miR-324-5p	4.867 79	0.000 10	rno-miR-664-3p	–1.398 99	0.000 02
rno-miR-532-5p	4.867 79	0.000 10	rno-miR-223-3p	–1.448 25	0
rno-miR-335	4.760 88	0.000 19	rno-miR-652-3p	–1.535 84	0
rno-miR-338-5p	4.760 88	0.000 19	rno-miR-1298	–1.861 81	0
rno-miR-129-5p	4.645 40	0.000 37	rno-miR-490-5p	–1.896 49	0
rno-miR-345-5p	4.645 40	0.000 37	rno-let-7e-3p	–1.980 59	0
rno-miR-380-3p	4.382 37	0.000 01	rno-miR-365-3p	–2.249 66	0
rno-miR-18a-5p	3.604 76	0	rno-miR-448-3p	–2.261 49	0.000 21
rno-miR-702-3p	3.230 36	0	rno-miR-1-3p	–2.361 03	0
rno-miR-760-3p	3.189 72	0	rno-miR-31a-5p	–2.524 52	0
rno-miR-3553	2.791 68	0	rno-miR-409b	–3.027 02	0.000 34
rno-miR-342-5p	2.723 40	0	rno-miR-3585-3p	–3.509 42	0
rno-miR-3559-3p	1.944 96	0	rno-miR-186-5p	–3.939 56	0.000 11
rno-miR-181a-1-3p	1.810 46	0	rno-miR-541-5p	–4.463 12	0
rno-miR-181a-2-3p	1.797 40	0.000 35	rno-miR-3588	–4.513 48	0
rno-let-7a-5p	1.649 62	0	rno-miR-3585-5p	–4.583 42	0
rno-miR-17-5p	1.423 01	0.000 05	rno-miR-764-5p	–4.640 00	0.000 28
rno-miR-103-3p	1.414 97	0	rno-miR-188-5p	–4.640 00	0.000 28
rno-miR-877	1.399 24	0.000 36	rno-miR-31a-3p	–4.640 00	0.000 28
rno-miR-449a-5p	1.331 46	0	rno-miR-500-3p	–4.640 00	0.000 28
rno-miR-211-5p	1.235 21	0	rno-miR-323-3p	–4.746 92	0.000 15
rno-miR-125b-5p	1.004 55	0	rno-miR-675-5p	–4.846 45	0.000 08
rno-miR-423-5p	–1.049 19	0	rno-miR-203b-5p	–4.846 45	0.000 08
rno-miR-100-5p	–1.055 04	0	rno-miR-487b-3p	–5.027 02	0.000 03
rno-miR-199a-3p	–1.080 42	0	rno-miR-219a-2-3p	–5.331 88	0
rno-miR-378a-3p	–1.106 46	0	rno-miR-3557-3p	–5.331 88	0
rno-miR-676	–1.122 43	0.000 04	rno-miR-450b-3p	–5.331 88	0
rno-miR-342-3p	–1.134 13	0	rno-miR-200c-5p	–5.331 88	0
rno-miR-126a-3p	–1.216 96	0	rno-miR-1306-3p	–5.640 00	0
rno-miR-145-5p	–1.252 72	0	rno-miR-330-3p	–6.149 02	0
rno-miR-185-5p	–1.253 22	0	rno-miR-3596a	–6.543 49	0
rno-miR-142-3p	–1.272 14	0.000 04	rno-miR-3570	–6.983 96	0
rno-miR-30a-3p	–1.297 22	0	rno-miR-183-5p	–11.816 08	0

Table 3
miRNA was differentially expressed between the COPD group (M) and COPD + ISZ group (D) (n =12).

Gene ID	$\log_2$ FC (M/D)	P-value (M/D)	Gene ID	$\log_2$ FC (M/D)	P-value (M/D)
rno-miR-125b-5p	7.772 15	0	rno-miR-142-3p	–1.137 74	0.000 29
rno-miR-181a-2-3p	6.354 11	0	rno-miR-224-5p	–1.208 63	0
rno-miR-3120	5.695 15	0	rno-miR-132-5p	–1.213 29	0.000 03
rno-miR-672-5p	5.617 14	0.000 01	rno-miR-130b-5p	–1.265 50	0.000 82
rno-miR-190b-5p	5.534 68	0.000 01	rno-miR-339-5p	–1.353 01	0
rno-miR-7b	5.254 57	0.000 06	rno-miR-652-3p	–1.369 84	0
rno-miR-129-5p	5.032 18	0.000 24	rno-miR-9a-5p	–1.522 41	0.000 57
rno-miR-345-5p	5.032 18	0.000 24	rno-miR-223-5p	–1.676 16	0.000 02
rno-miR-674-5p	4.970 78	0	rno-miR-490-5p	–1.694 14	0
rno-miR-107-3p	4.769 15	0.000 95	rno-miR-144-3p	–1.762 23	0
rno-miR-3084a-5p	4.769 15	0.000 95	rno-miR-365-3p	–1.943 69	0
rno-miR-17-5p	4.617 14	0	rno-miR-223-3p	–1.944 33	0
rno-miR-301a-3p	4.091 08	0	rno-miR-664-3p	–2.055 28	0
rno-miR-196a-5p	3.447 22	0	rno-miR-23b-5p	–2.318 31	0.000 09
rno-miR-214-3p	3.125 29	0	rno-miR-1-3p	–2.345 34	0
rno-miR-3596b	3.058 65	0	rno-miR-138-5p	–2.450 90	0
rno-miR-3556b	2.406 58	0	rno-miR-672-3p	–2.588 40	0
rno-miR-877	2.288 52	0	rno-miR-3585-3p	–3.137 74	0
rno-miR-582-5p	2.032 18	0.000 18	rno-miR-31a-5p	–3.342 86	0
rno-miR-18a-5p	1.991 54	0.000 03	rno-miR-350	–3.640 24	0.000 60
rno-let-7a-5p	1.940 70	0	rno-miR-186-5p	–3.800 71	0.000 21
rno-miR-3068-5p	1.921 15	0	rno-miR-369-5p	–4.012 21	0.000 05
rno-miR-1949	1.883 32	0	rno-miR-3588	–4.300 88	0
rno-miR-708-5p	1.777 87	0	rno-miR-3594-5p	–4.552 78	0.000 36
rno-miR-326-3p	1.744 90	0	rno-miR-324-3p	–4.597 17	0
rno-miR-181a-1-3p	1.702 48	0	rno-miR-31a-3p	–4.722 71	0.000 13
rno-miR-143-3p	1.531 28	0.000 02	rno-miR-500-3p	–4.800 71	0.000 08
rno-miR-3559-3p	1.508 62	0.000 05	rno-miR-124-3p	–5.012 21	0.000 02
rno-miR-497-5p	1.388 33	0.000 13	rno-miR-9a-3p	–5.076 34	0.000 01
rno-miR-196b-5p	1.305 20	0.000 06	rno-miR-3557-3p	–5.253 22	0
rno-miR-27a-5p	1.281 21	0.001 00	rno-miR-30c-2-3p	–5.307 67	0
rno-miR-187-3p	1.245 59	0.000 01	rno-miR-384-5p	–5.410 76	0
rno-miR-122-5p	1.221 66	0	rno-miR-764-5p	–5.459 67	0
rno-miR-342-5p	1.140 56	0.000 04	rno-miR-330-3p	–5.597 17	0
rno-miR-146a-5p	–1.022 28	0	rno-miR-532-3p	–5.874 71	0
rno-miR-30c-5p	–1.023 98	0	rno-miR-874-3p	–5.979 04	0
rno-miR-322-5p	–1.062 80	0	rno-miR-3570	–6.012 21	0
rno-miR-206-3p	–1.076 34	0.000 03	rno-miR-3596a	–6.489 50	0
rno-miR-128-3p	–1.127 02	0	rno-miR-183-5p	–9.947 24	0

Table 4
Differentially expressed miRNAs from different groups (n = 12).

Gene ID	K expression	D expression	M expression	$\log_2$ FD (M/K)	$\log_2$ FD (M/D)	Q value (K *vs.* M)	Q value (D *vs.* M)
rno-miR-672-5p	0	0	9.0	5.230 36	5.617 14	0.000 03	0.000 01
rno-miR-190b-5p	0	0	8.5	5.147 90	5.534 68	0.000 05	0.000 01
rno-miR-129-5p	0	0	6.0	4.645 40	5.032 18	0.000 91	0.000 24
rno-miR-345-5p	0	0	6.0	4.645 40	5.032 18	0.000 91	0.000 24
rno-miR-1-3p	35.0	46.5	6.5	–2.361 03	–2.345 34	0	0
rno-miR-31a-5p	17.5	35.0	3.0	–2.524 52	–3.342 86	0.000 01	0
rno-miR-3585-3p	46.0	45.5	4.0	–3.509 42	–3.137 74	0	0
rno-miR-186-5p	8.0	9.5	0.5	–3.939 56	–3.800 71	0.000 32	0.000 21
rno-miR-3588	782.5	858.5	35.0	–4.513 48	–4.300 88	0	0
rno-miR-31a-3p	6.5	8.0	0	–4.640 00	–4.722 71	0.000 74	0.000 13
rno-miR-500-3p	5.0	8.5	0	–4.640 00	–4.800 71	0.000 74	0.000 08
rno-miR-764-5p	6.0	13.0	0	–4.640 00	–5.459 67	0.000 74	0
rno-miR-3557-3p	10.0	12.0	0	–5.331 88	–5.253 22	0.000 01	0
rno-miR-330-3p	16.5	12.0	0	–6.149 02	–5.597 17	0	0
rno-miR-3596a	6 116.5	7 141.0	72.5	–6.543 49	–6.489 50	0	0
rno-miR-3570	29.5	21.5	0	–6.983 96	–6.012 21	0	0
rno-miR-183-5p	851.5	294.0	0	–11.816 08	–9.947 24	0	0

Note: K represents control group, M represents COPD group, and D represents COPD + ISZ group.

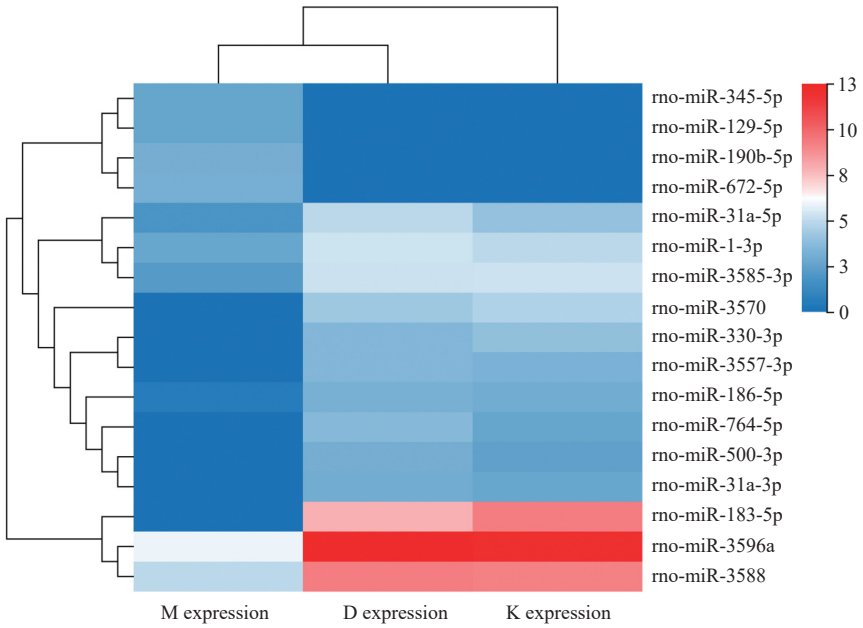

Fig. 4 Cluster analysis of 17 differentially expressed miRNAs. Red color represents a relative high expression level. Blue color shows a relative low expression level.

by different software are shown in Table S4. Then select the intersection of the prediction results of different software for further analysis.

To understand the functional role of target genes, we further performed GO and KEGG enrichment analysis on the common regions obtained from the 3 software. GO consists of 3 main bodies, including molecular function (MF), biological process (BP), and cellular component (CC). These functional entries in GO indicate the biological function and signal correlation of target genes corresponding to differentially expressed miRNAs. The results showed that the target gene functions of different miRNAs were mainly BP, mainly manifested in cell part, organelle, binding and cellular process. KEGG pathway analysis has enriched the potential pathway for gene prediction. Among them, the important pathways include axon guidance, mitogen-activated protein kinase (MAPK) signaling pathway, AMP-activated protein kinase (AMPK) signaling pathway, and metabolic pathway (Fig. 5).

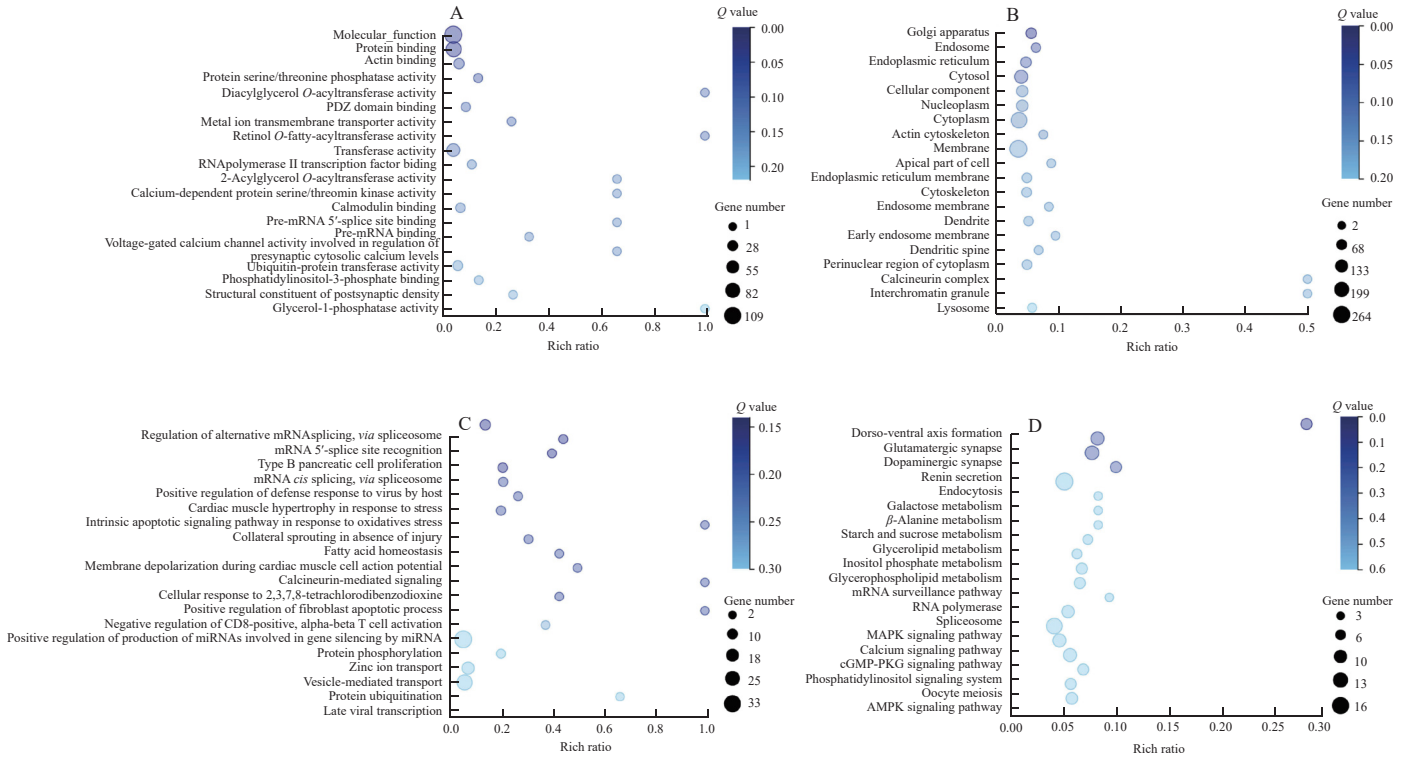

Fig. 5 GO and KEGG enrichment analysis. (A) GO analysis in molecular function. (B) GO analysis in cellular components. (C) GO analysis in biological processes. (D) KEGG pathways of top 20 enrichment score.

3.7 Validation of expression of miRNAs

In order to verify the results of sequencing data, qRT-PCR based on TaqMan was used to detect and 4 miRNAs differentially expressed in the high-throughput sequencing results were selected for verification. The primer sequence is shown in Table S5. The expression results are shown in Fig. 6. The results showed that the expression of miR-672-5p, miR-190b-5p, miR-129-5p and miR-345-5p were all low in the control group and high in the COPD group, and the expression of the 4 miRNAs was significantly downregulated after the drug treatment which was consistent with the sequencing results. This indicates that the sequencing results are reliable.

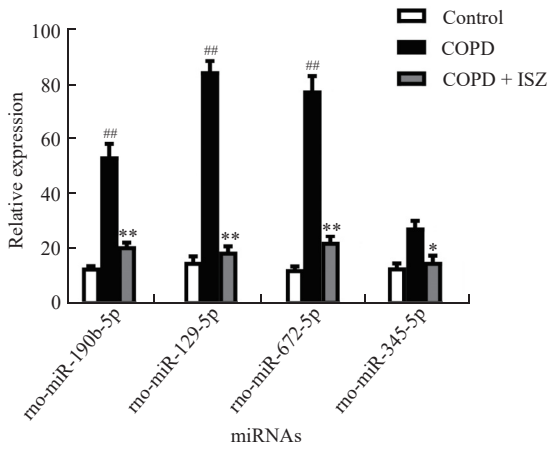

Fig. 6 Verification results of qRT-PCR.The expressions of the 4 miRNAs were all low in the control group and high in the COPD group. The expressions of the 4 miRNAs were significantly down-regulated after drug treatment. Data are presented as mean ± SEM difference of three independent experiments. $^{\#\#}P < 0.01$ compared with the control group; $^{*}P < 0.05$ and $^{**}P < 0.01$ compared with the control group.

4. Discussion

Coronary obstructive pulmonary disease is a very prevailing disease. As per recent data on COPD, it is the third most common cause of death across the globe[31]. The disease includes small air pathway disorders, emphysema, and chronic bronchitis, which can be caused by environmental exposure, mainly smoking[32]. In recent years, miRNAs in tissues and body fluids have become a promising biomarker for a variety of diseases. Biomarkers in blood have been particularly popular in recent years because serum or plasma is readily available and can be repeatedly sampled[9,33]. Several different types of miRNAs have been found closely associated with asthma related inflammation[34]. In this context, miRNAs possess very high potential for diagnostic and therapeutic value. Though several limitations in profiling methods, miRNA profiling has its due advantages over other conventional detective techniques[35]. It not only reveals that the pathogenesis of COPD is closely related to the abnormal expression of miRNA, providing a new biomarker for the prediction and early detection of COPD[36], but also provides a new idea for studying the pathogenesis of COPD or airway epithelial injury[37].

The formation of COPD was determined by the pathological changes of rat lung tissue. In this study, high-throughput sequencing and bioinformatics analysis were combined to explore the influence of miRNA expression profiles in rat serum exosomes. Previous studies have shown that extracts from ISZ have a good therapeutic effect on COPD[38]. Exosomes were extracted from serum of normal rats, COPD rats and ISZ drug intervention COPD rats. Comparison of miRNA expression levels between the COPD group and control group showed that 72 miRNAs were differentially expressed in exosomes. These included 25 up-regulated and 47 down-regulated miRNAs, suggesting that these 72 miRNAs may be associated with COPD and that they may be biomarkers of COPD. Comparison of miRNA expression profiles between the COPD group and the COPD + ISZ group showed that 34 miRNAs were up-regulated and 44 miRNAs were down-regulated. In order to confirm that the extract of ISZ regulates the disease by affecting the expression of serum exosomes, we further analyzed the cross-over miRNAs, 17 of which showed significant differences during drug administration intervention, among which 4 were up-regulated and 13 were down-regulated. From 17 shortlisted miRNAs, majorly expressive miRNAs were then further evaluated *via* qRT-PCR that confirmed the differentially high expression of miR-190b-5p, miR-345-5p, miR-672-5p and miR-129-5p. Therefore, these 4 miRNAs have greater potential for the consideration as diagnostic and prognostic biomarkers against COPD. Interestingly, our findings concluded that these (miR-672-5p, miR-190b-5p, miR-129-5p and miR-345-5p) were significantly downregulated in the COPD + ISZ group indicating not only its relevancy but also the efficacy of ISZ against COPD. ISZ may reduce the expression of these 4 miRNAs in the treatment of COPD. The results indicated that the composition of serum exosomes in COPD rats was significantly different from that in normal rats. The corresponding variations in the expression of serum exosome miRNA are linked with COPD and these 17 shortlisted miRNAs possess strong potential to qualify for the choice of COPD associated biomarkers.

The diagnosis of several human diseases has become quite conventional through high-throughput sequencing. Next-generation sequencing has enhanced the capabilities of medical science to narrow down the disease associated genes. At present, no marker of COPD with 100% sensitivity and specificity has been found, and how these miRNA affects the occurrence of the disease through expression remains unclear, which needs further in-depth research. From the family of Labiatae, ISZ of genus *Camellia*, is an herbal plant from traditional Chinese medicine. The plant is very famous for its edibility among Chinese community because of its nutritious and therapeutic importance[38]. Because of the presence of triterpenoids and sterols, several diseases have been reported to be potentially treatable with ISZ extract including, viral and bacterial infections as well as inflammatory and tumor diseases. Additionally, a very recent study has reported the potential therapeutic efficacy of ISZ against COPD[19]. Our earlier studies have published a comprehensive report on the active ingredients from ISZ chiefly including Glaucocalyxin A (GLA)[39]. It is worth noticing that GLA has the vast majority of herbs of the genus *Camellia*. Most pharmacological effects, such as anti-inflammatory, antibacterial, anticancer, antioxidant, antithrombotic and so on[40].

Circulating RNA has been documented as a potential diagnostic biomarker for a variety of diseases[41], including COPD. The results showed that the up-regulation of miR-672-5p, miR-190b-5p, miR-129-5p and miR-345-5p was closely related to COPD. The decreased expression of miR-627-5p may have an inhibitory effect on hepatocellular carcinoma, possibly through a transcriptional coactivator targeting recombinant B-cell CLL/lymphoma 3 (BCL3). miR-627-5p inhibited cell proliferation, delayed migration and promoted cell apoptosis by

increasing Y-box binding protein 2 (YBX2) expression in oral squamous cell carcinoma[42]. miR-627-5p is associated with pathways related to myocardial hypertrophy, cardiomyocyte differentiation, proliferation, and P2Y purine signal transduction[43]. miR-190 is a microRNAs involved in the regulation of neuroinflammation, which can improve tumor formation and lung metastasis capacity of human hepatocellular carcinomas (HepG2) cells. Stable overexpression of miR-190 leads to downregulation of PH domain and leucine rich repeat protein phosphatase 1 (PHLPP1) protein[44], thus it possess good potential as a therapeutic and diagnostic target for hepatocellular carcinoma. Overexpression of miR-190 itself can enhance cell proliferation and malignant transformation, enhance protein kinase B (Akt) activation and vascular endothelial growth factor expression[45]. microRNA-129-5p (miR-129-5p) regulates cell proliferation and invasion in lung cancer. Its abnormal expression has been detected in various types of human cancer, and the validated target genes are involved in cancer-related biological processes such as cell proliferation, apoptosis, cell cycle, and metastasis, regulating a wide range of biological functions[46]. miR-129-5p plays an important role in tumorigenesis and acts by promoting or inhibiting tumors[47]. It is a potential therapeutic agent because of its association with apoptosis, cell cycle and chemical resistance. miR-345-5p can inhibit the malignant phenotype of lung adenocarcinoma cells by inhibiting cell proliferation, migration, invasion and promoting cell apoptosis, and miR-345-5p can inhibit the migration and invasion of lung adenocarcinoma cells by regulating ras homolog gene family, member A (RhoA) to induce cell apoptosis[48]. Overall, our studies have found that chronic obstructive pulmonary disease was very much linked with high expression of miR-190b-5p, miR-345-5p, miR-129-5p and miR-672-5p.

Concluding the studies after employing a mix of *in silico*, *in vitro* and *in vivo* experimental techniques, we were converged towards COPD related 17 different miRNAs from serum exosomes. Out of which 4 miRNA targets (miR-190b-5p, miR-345-5p, miR-129-5p and miR-672-5p) have strong predictive, prognostic and therapeutic potential against COPD. Additionally, it was also concluded that extract from ISZ leaves has convincing potential to treat the disease by regulating COPD associated miRNA that also explains the mechanism of the treatment of COPD by ISZ leaves extract.

Conflict of interest

Zhaojun Wei is an editorial board member for *Food Science and Human Wellness* and was not involved in the editorial review or the decision to publish this article. The authors have nothing to declare.

Acknowledgements

This work was supported by the National Natural Science Foundation of China (82170481, 82570069), Anhui Natural Science Foundation (2008085J39 and 2108085MH314), Anhui Province Innovation Team of Authentic Medicinal Materials Development and High Value Utilization (2022AH010080), and Suzhou University Joint Cultivation Postgraduate Research Innovation Fund Project (2023KYCX04).

Appendix A. Supplementary information

Supplementary data associated with this article can be found, in the online version, at http://doi.org/10.26599/FSHW.2024.9250250.

Reference

[1] J.B. Soriano, F. Polverino, B.G. Cosio, What is early COPD and why is it important? Eur. Respir J. 52 (2018) 1801448. https://doi.org/10.1183/13993003.01448-2018.

[2] K.F. Rabe, H. Watz, Chronic obstructive pulmonary disease, Lancet 389 (2017) 1931-1940. https://doi.org/10.1016/S0140-6736(17)31222-9.

[3] J.L. Schneider, J.H. Rowe, C. Garcia-de-Alba, et al., The aging lung: physiology, disease, and immunity, Cell 184 (2021) 1990-2019. https://doi.org/10.1016/j.cell.2021.03.005.

[4] K. Mycroft, R. Krenke, K. Górska, Eosinophils in COPD-current concepts and clinical implications, J. Allergy Clin. Immunol. Pract. 8 (2020) 2565-2574. https://doi.org/10.1016/j.jaip.2020.03.017.

[5] R. Shi, C. Huang, Y. Gao, et al., Gut microbiota axis: potential target of phytochemicals from plant-based foods, Food Sci. and Hum. Wellness 12 (2023) 1409-1426. https://doi.org/10.1016/j.fshw.2023.02.001.

[6] X. Liu, X. Zhang, Y. Gao, et al., Cyanidin-3-galactoside from *Aronia melanocarpa* ameliorates PM10-induced pulmonary inflammation by promoting PINK1/Parkin signaling pathway-mediated alveolar macrophage mitophagy, eFood 4 (2023) e119. https://doi.org/10.1002/efd2.119.

[7] W. Rao, S. Wang, M. Duleba, S. et al., Regenerative metaplastic clones in COPD lung drive inflammation and fibrosis, Cell 181 (2020) 848-864. https://doi.org/10.1016/j.cell.2020.03.047.

[8] M. Yin, X. Ding, S. Yin, L. et al., Exosomes from hepatitis B virus-infected hepatocytes activate hepatic stellate cells and aggravate liver fibrosis through the miR-506-3p/Nur77 pathway, J. Biochem. Mol. Toxicol. 37 (2023) e23432. https://doi.org/10.1002/jbt.23432.

[9] M.A. Mori, R.G. Ludwig, R. Garcia-Martin, et al., Extracellular mirnas: from biomarkers to mediators of physiology and disease, Cell Metab. 30 (2019) 656-673. https://doi.org/10.1016/j.cmet.2019.07.011.

[10] B.X. He, Z.Y. Zhao, Q.D. Cai, et al., miRNA-based biomarkers, therapies, and resistance in cancer, Int. J. Biol. Sci. 16 (2020) 2628-2647. https://doi.org/10.7150/ijbs.47203.

[11] L. Zhou, W. Wang, F. Wang, et al., Plasma-derived exosomal miR-15a-5p as a promising diagnostic biomarker for early detection of endometrial carcinoma, Mol. Cancer 20 (2021) 57. https://doi.org/10.1186/s12943-021-01352-4.

[12] K.F. Zhai, H. Duan, Y. Shi, et al., miRNAs from plasma extracellular vesicles are signatory noninvasive prognostic biomarkers against atherosclerosis in LDLr$^{-/-}$ mice, Oxid. Med. Cell Longev. 2022 (2022) 6887192. https://doi.org/10.1155/2022/6887192.

[13] J. Wang, C. Jiang, N. Li, et al., The circEPSTI1/mir-942-5p/LTBP2 axis regulates the progression of OSCC in the background of OSF *via* EMT and the PI3K/Akt/mTOR pathway, Cell Death Dis. 11 (2020) 682. https://doi.org/10.1038/s41419-020-02851-w.

[14] J. Wang, J. Ge, Y. Wang, F. miRNAs BART et al., 11 and BART17-3p promote immune escape through the enhancer-mediated transcription of PD-L1, Nat. Commun. 13 (2022) 866. https://doi.org/10.1038/s41467-022-28479-2.

[15] G. Zhang, M. Li, H. Deng, et al., SGNNMD: signed graph neural network for predicting deregulation types of miRNA-disease associations, Brief. Bioinform. 23 (2022) bbab464. https://doi.org/10.1093/bib/bbab464.

[16] I.K. Sundar, D. Li, I. Rahman, Small RNA-sequence analysis of plasma-derived extracellular vesicle miRNAs in smokers and patients with chronic obstructive pulmonary disease as circulating biomarkers, J. Extracell. Vesicles 8 (2019) 1684816. https://doi.org/10.1080/20013078.2019.1684816.

[17] W. Wang, H. Li, J. Lyu, et al., Determination of the anti-oxidative stress mechanism of Isodon suzhouensis leaves by employing bioinformatic and novel research technology, ACS Omega 8 (2023) 3520-3529. https://doi.org/10.1021/acsomega.2c07913.

[18] X. Chen, X. Dai, Y. Liu, et al., *Isodon rubescens* (Hemls.) Hara.: a comprehensive review on traditional uses, phytochemistry, and

pharmacological activities, Front. Pharmacol. 13 (2022) 766581. https://doi.org/10.3389/fphar.2022.766581.

[19] H. Duan, W. Wang, S. Li, et al., The potential mechanism of *Isodon suzhouensis* against COVID-19 *via* EGFR/TLR4 pathways. Food Sci. Hum. Wellness 13 (2024) 3245-3255. https://doi.org/10.26599/FSHW.2023.9250011.

[20] H. Duan, G.C. Wang, G.J. Khan, et al., Identification and characterization of potential antioxidant components in *Isodon amethystoides* (Benth.) Hara tea leaves by UPLC-LTQ-Orbitrap-MS, Food Chem. Toxicol. 148 (2021) 111961. https://doi.org/10.1016/j.fct.2020.111961.

[21] S. Liang, X. Meng, Z. Wang, et al., Polysaccharide from *Ephedra sinica* Stapf inhibits inflammation expression by regulating Factor-β1/Smad2 signaling, Int. J. Biol. Macromol. 106 (2018) 947-954. https://doi.org/10.1016/j.ijbiomac.2017.08.096.

[22] L. Dong, Y. Wang, T. Zheng, et al., Hypoxic hUCMSC-derived extracellular vesicles attenuate allergic airway inflammation and airway remodeling in chronic asthma mice, Stem. Cell Res. Ther. 12 (2021) 4. https://doi.org/10.1186/s13287-020-02072-0.

[23] K. Zhai, H. Duan, W. Wang, et al., Ginsenoside Rg1 ameliorates blood-brain barrier disruption and traumatic brain injury *via* attenuating macrophages derived exosomes miR-21 release, Acta Pharm. Sin. B 11 (2021) 3493-3507. https://doi.org/10.1016/j.apsb.2021.03.032.

[24] A. Shang, C. Gu, W. Wang, et al., Exosomal circPACRGL promotes progression of colorectal cancer *via* the miR-142-3p/miR-506-3p-TGF-β1 axis, Mol. Cancer 19 (2020) 117. https://doi.org/10.1186/s12943-020-01235-0.

[25] M. Hong, S. Tao, L. Zhang, et al., RNA sequencing: new technologies and applications in cancer research, J. Hematol. Oncol. 13 (2020) 166. https://doi.org/10.1186/s13045-020-01005-x.

[26] Z. Li, J. Wu, W. Wei, et al., Association of serum miR-186-5p with the prognosis of acute coronary syndrome patients after percutaneous coronary intervention, Front. Physiol. 10 (2019) 686. https://doi.org/10.3389/fphys.2019.00686.

[27] T. Hennig, A.B. Prusty, B.B. Kaufer, et al., Selective inhibition of miRNA processing by a herpesvirus-encoded miRNA, Nature 605 (2022) 539-544. https://doi.org/10.1038/s41586-022-04667-4.

[28] K. Inoue, N. Ogonuki, S. Kamimura, et al., Loss of H3K27me3 imprinting in the Sfmbt2 miRNA cluster causes enlargement of cloned mouse placentas, Nat. Commun. 11 (2020) 2150. https://doi.org/10.1038/s41467-020-16044-8.

[29] B. Zhou, K. Xu, X. Zheng, et al., Application of exosomes as liquid biopsy in clinical diagnosis, Signal Transduct. Target. Ther. 5 (2020) 144. https://doi.org/10.1038/s41392-020-00258-9.

[30] T. Liu, Q. Zhang, J. Zhang, et al., EVmiRNA: a database of miRNA profiling in extracellular vesicles, Nucleic Acids Res. 47 (2019) D89-D93. https://doi.org/10.1093/nar/gky985.

[31] C. Viniol, C.F. Vogelmeier, Exacerbations of COPD, Eur. Respir. Rev. 27 (2018) 170103. https://doi.org/10.1183/16000617.0103-2017.

[32] M.C. Basil, F.L. Cardenas-Diaz, J.J. Kathiriya, et al., Human distal airways contain a multipotent secretory cell that can regenerate alveoli, Nature 604 (2022) 120-126. https://doi.org/10.1038/s41586-022-04552-0.

[33] J.N. Vo, M. Cieslik, Y. Zhang, et al., The landscape of circular RNA in cancer, Cell 176 (2019) 869-881. https://doi.org/10.1016/j.cell.2018.12.021.

[34] K.R. Genschmer, D.W. Russell, C. Lal, et al., Activated PMN exosomes: pathogenic entities causing matrix destruction and disease in the lung, Cell 176 (2019) 113-126.e15. https://doi.org/10.1016/j.cell.2018.12.002.

[35] J. Yue, Z.S. Chen, X.X. Xu, et al., Functions and therapeutic potentials of exosomes in osteosarcoma, Acta Mater. Med. 1 (2022) 552-562. https://doi.org/10.15212/amm-2022-0024.

[36] J. Huang, W. Jiang, X. Tong, et al., Identification of gene and microRNA changes in response to smoking in human airway epithelium by bioinformatics analyses, Medicine 98 (2019) e17267. https://doi.org/10.1097/MD.0000000000017267.

[37] Q. Yu, D. Yang, X. Chen, et al., CD147 increases mucus secretion induced by cigarette smoke in COPD, BMC Pulm. Med. 19 (2019) 29. https://doi.org/10.1186/s12890-019-0791-0.

[38] K.F Zhai, W. Wang, M.Q. Zheng, et al., Protective effects of *Isodon Suzhouensis* extract and glaucocalyxin A on chronic obstructive pulmonary disease through SOCS3-JAKs/STATs pathway, Food Front. 4 (2023) 511-523. https://doi.org/10.1002/fft2.177.

[39] J. Zhu, Y. Sun, Y. Lu, et al., Glaucocalyxin A exerts anticancer effect on osteosarcoma by inhibiting GLI1 nuclear translocation *via* regulating PI3K/Akt pathway, Cell Death Dis. 9 (2018) 708. https://doi.org/10.1038/s41419-018-0684-9.

[40] W. Zhu, Y. Zhang, Y. Li, et al., Glaucocalyxin A attenuates IL-1β-induced inflammatory response and cartilage degradation in osteoarthritis chondrocytes *via* inhibiting the activation of NF-κB signaling pathway, Dis. Markers 2022 (2022) 6516246. https://doi.org/10.1155/2022/6516246.

[41] Y. Yuan, R. Yuan, Q. Xin, et al., Tetramethylpyrazine and paeoniflorin combination (TMP-PF) inhibits angiogenesis in atherosclerosis *via* miR-126/VEGF/VEGFR2 signaling pathway, J. Future Foods 4 (2024) 280-287. https://doi.org/10.1016/j.jfutfo.2023.07.010.

[42] E.C. Tuysuz, U. Ozbey, S. Gulluoglu, et al., miRNAs as cell fate determinants of lateral and paraxial mesoderm differentiation from embryonic stem cells, Dev. Biol. 478 (2021) 212-221. https://doi.org/10.1016/j.ydbio.2021.07.002.

[43] D.Y. Zhao, L. Zhou, T.F. Yin, et al., Circulating miR-627-5p and miR-199a-5p are promising diagnostic biomarkers of colorectal neoplasia, World J. Clin. Cases 10 (2022) 5165-5184. https://doi.org/10.12998/wjcc.v10.i16.5165.

[44] Y. Xiong, S. Wu, H. Yu, et al., miR-190 promotes HCC proliferation and metastasis by targeting PHLPP1, Exp. Cell Res. 371 (2018) 185-195. https://doi.org/10.1016/j.yexcr.2018.08.008.

[45] K. Beezhold, J. Liu, H. Kan, et al., miR-190-mediated downregulation of PHLPP contributes to arsenic-induced Akt activation and carcinogenesis, Toxicol. Sci. 123 (2011) 411-420. https://doi.org/10.1093/toxsci/kfr188.

[46] C. Xu, Z. Du, S. Ren, et al., MiR-129-5p sensitization of lung cancer cells to etoposide-induced apoptosis by reducing YWHAB, J. Cancer 11 (2020) 858-866. https://doi.org/10.7150/jca.35410.

[47] W. Luo, J. Wang, W. Xu, et al., LncRNA RP11-89 facilitates tumorigenesis and ferroptosis resistance through PROM2-activated iron export by sponging miR-129-5p in bladder cancer, Cell Death Dis. 12 (2021) 1043. https://doi.org/10.1038/s41419-021-04296-1.

[48] Q.Y. Zhou, S.Y. Gui, P. Zhang, et al., Upregulation of miR-345-5p suppresses cell growth of lung adenocarcinoma by regulating ras homolog family member A (RhoA) and Rho/Rho associated protein kinase (Rho/ROCK) pathway, Chin. Med. J. (Engl.) 134 (2021) 2619-2628. https://doi.org/10.1097/CM9.0000000000001804.